

Preformed Particle Gel for Conformance Control: Transport Mechanism Through Porous Media

Baojun Bai, SPE, U. of Missouri-Rolla, and Yuzhang Liu, SPE, J.-P. Coste, and Liangxiong Li, SPE, Research Inst. of Petroleum Exploration and Development, PetroChina

Summary

Preformed particle gel (PPG) has been successfully synthesized and applied to control excess water production in most of the mature, waterflooded oil fields in China. This paper reports on laboratory experiments carried out to investigate PPG transport mechanisms through porous media. Visual observations in etched-glass micromodels demonstrate that PPG propagation through porous media exhibits six patterns of behavior: direct pass, adsorption, deform and pass, snap-off and pass, shrink and pass, and trap. At the macroscopic scale, PPG propagation through porous media can be described by three patterns: pass, broken and pass, and plug. The dominant pattern is determined by the pressure change with time along a tested core (as measured at specific points), the particle-size ratio of injected and produced particles from the core outlet, and the residual resistance factor of each segment along the core. Measurements from micromodel and routine coreflooding experiments show that a swollen PPG particle can pass through a pore throat with a diameter that is smaller than the particle diameter owing to the elasticity and deformability of the swollen PPG particle. The largest diameter ratio of a PPG particle and a pore throat that the PPG particle can pass through depends on the swollen PPG strength. PPG particles can pass through porous media only if the driving pressure gradient is higher than the threshold pressure gradient. The threshold pressure depends on the strength of the swollen PPG and the ratio of the particle diameter and the average pore diameter.

Introduction

Reservoir heterogeneity is a principle factor responsible for the low sweep efficiency of injected water or gas. To control conformance in waterflooding or gasflooding, many technologies have been applied, such as polymer flooding, foam flooding, alkaline-surfactant-polymer (ASP), and so on (Wang et al. 2003; Song et al. 1995; Grigg and Schechter 1997). Injecting a large volume of gel to correct in-depth permeability for those reservoirs with fractures or channels has been an attractive technology for years (Sydansk and Southwell 2000; Lane and Seright 2000; Wang et al. 2001; Fielding et al. 1994; Bai et al. 1999). In this paper, "channel" means a super-high-permeability zone or streak; it does not mean flow through a common matrix.

In recent years, the study of preformed gel for conformance control has gained great interest among gel-based enhanced-oil-recovery processes. Seright (1997, 2000) studied the behavior of preformed bulk gel through fractures and demonstrated that preformed bulk gel had better placement than in-situ gel and could effectively reduce gel damage on unswept low-permeability oil zones or matrix (Seright 1997, 2000, 2003; Chauveteau et al. 2000, 2001). Chauveteau et al. (2000, 2001, 2003) synthesized preformed microgel particles that were crosslinked under shear; Feng et al. (2003) demonstrated that the microgels could be easily injected into porous media without any sign of plugging, and that

these microgels should be good candidates for water-shutoff and profile-control operations.

PPG is another kind of preformed gel; it is also a particle gel and was developed by the authors of this paper according to the following procedures:

1. Bulk gel was synthesized using an acrylamide monomer, a crosslinker, an initiative, and additives at room temperature in surface facilities.

2. The bulk gel was cut into particles with a cutting machine.

3. The cut particles were dried at a higher temperature to form xerogel particles.

4. The dried particles were ground and sieved according to the requirement of specified reservoirs.

This process provides an easily packed product. The advantages of PPG for conformance control are summarized as follows (Coste et al. 2000; Bai et al. 2004; Liu et al. 1999):

- PPG, synthesized in surface facilities, can overcome some distinct drawbacks inherent in in-situ gelation systems, such as lack of gelation time, uncertainty of gelling due to shear, degradation, chromatographic fractionation or change of gelant compositions, and dilution by formation water.

- PPG is strength- and size-controlled, environmentally friendly, thermostable, and not sensitive to reservoir minerals or formation water salinity.

- PPG can resist temperatures up to 120°C and salinity up to 300,000 mg/L.

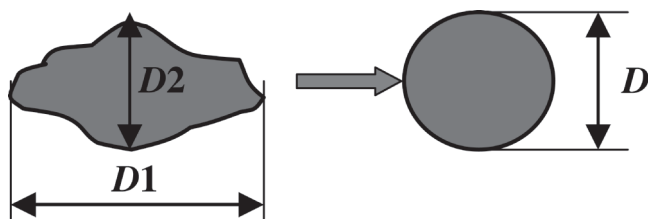
- PPG suspensions can be prepared using produced water, which can save fresh water and protect the environment.

- PPG injection operation processes and surface facilities are simple, which can reduce operation and labor costs.

PPG has been applied to control conformance in most of the mature oil fields in China, and most of the PPG applications have shown positive results (Liu et al. 2006). In this research, laboratory experiments, including visual micromodel and coreflooding tests, were conducted to deduce the mechanisms of PPG transport through porous media.

Experimental Methods

PPG. The tested PPG product was synthesized in our laboratory. The detailed synthesis procedure was reported in our other paper (Bai et al. 2004). Two kinds of PPG particles were selected for our experiments. PPG suspensions were prepared by mixing the particles with tap water from Beijing. Swelling capacity and strength were evaluated for the two types of PPG. The swelling capacity was defined as the ratio of the swollen particle mass to the dried particle mass. The swelling capacities of the two samples are 74 and 30, respectively, at 25°C. The strength of PPG was scaled by visually inspecting a large fully swollen particle flow through a tube, as proposed by Sydansk (1988). The first type, Sample 1, is a moderately flowing gel, and the second type, Sample 2, is a moderately deformable nonflowing gel. For convenience, Sample 1 is referred to as "weak particle," and Sample 2 is referred to as "strong particle" in this paper. In addition, these particles are irregular, so the equivalent diameter of a PPG particle is defined as the diameter of a circle that has the same projected area on a plane as the PPG particle, shown in **Fig. 1**. PPG cannot be dissolved in water, so the mixture of water and PPG is called PPG suspension.



$$S_{\text{particle}} = S_{\text{circle}}$$

$$D = \sqrt{\frac{4S_{\text{particle}}}{\pi}}$$

Fig. 1—The definition of particle diameter.

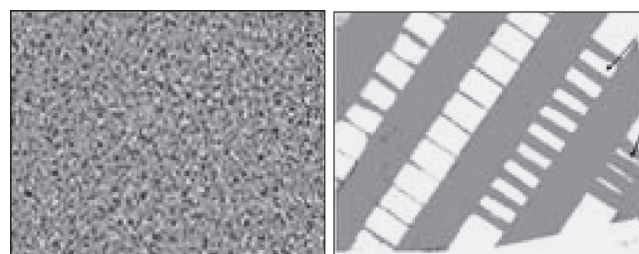
In this paper, the particle size of a sample refers to the average equivalent diameter of 100 dry particles, which are randomly selected from the sample. The particles used in the experiment have a normal-size distribution.

Etched Glass Micromodels. A micromodel is the transparent network of pores and constrictions that simulates the complexities of natural porous media. In our experiments, two patterns of micromodels were used: irregular models and simplified regular pore models, shown in Fig. 2. All models were fabricated using a photolithographic process and were water-wet (Morrow 1991; Chambers 1990).

The etched patterns of irregular models were based on amplificatory thin sections of sandstone from Daqing oil field, China, shown in Fig. 2a. The thin sections were enlarged to several times their original sizes because the original pore throats of these sections were so small that PPG particles could not be injected. The irregular models were used to study PPG propagation behaviors through porous media. The models were fabricated using two pieces of 0.2-cm glass plate. The plate size is 4.5 × 4.5 cm. The pattern size is 3 × 3 cm, and the pore cross sections are 50 to 300 μm with a pore depth of 5 to 100 μm.

The etched patterns of the simplified regular models (Fig. 2b) are based on our special design. These models were used to study the mechanism of PPG transportation through porous media and the matching ratio of a pore-throat diameter and a particle size. The plate and pattern size of these models are the same as those of the irregular models, except that their pore-throat sizes are different. In this kind of model, the pore throats are aligned in what is called a line, and the pore space is represented by an open column (Fig. 3). These models each have several lines, each with different pore-throat sizes, but all pore-throat sizes are the same size for the same line. In these models, the pore throats decrease in size from the entrance to the middle and increase from the middle to the outlet, with the smallest pore throats located in a single line in the middle of the micromodel. Table 1 lists the pore-throat size of each line from the entrance to the middle. The depth of a pore throat is the same as its width.

Single Sandpacked Core Model. Quartz sands with different sizes were packed in a stainless steel tube with two pressure taps, shown in Fig. 4. Tap I is an injection point, and Tap B is the point in the middle of the core. The outlet D of the core is open to atmosphere. Quartz sizes (from 20 to 100 meshes) are dependent on the permeability requirement of different experiments. The length of the tube is 30 cm, and its diameter is 2.2 cm. The sandpacked core models were used to study the matching ratio of particle diameter and average pore diameter of porous media (that is, what size of particles can pass through what size of pore throats in porous media). Table 2 gives the basic parameters for the models packed with different quartz sizes.



(a) Real core model used for irregular network model (b) Specified designed simple network model

Fig. 2—Schematic charts of micromodels.

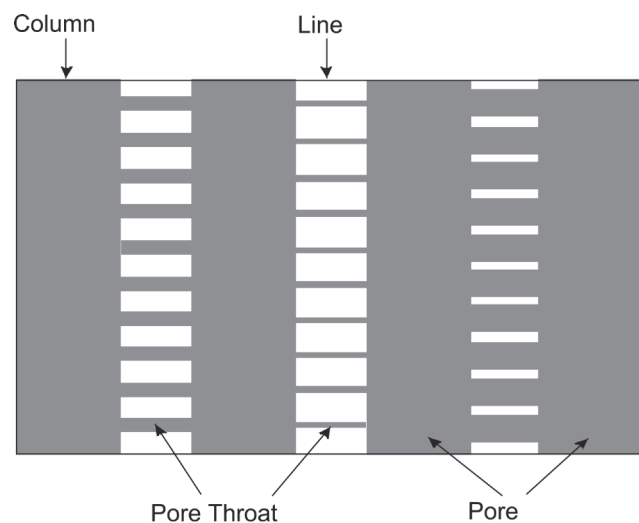


Fig. 3—Definitions of “line” and “column.”

TABLE 1—PORE-THROAT SIZES OF SIMPLIFIED REGULAR MICROMODELS

| Line No. | 1 | 2 | 3 | 4 |
|---------------------------|-----|----|----|----|
| Pore-throat diameter (μm) | 250 | 90 | 55 | 33 |

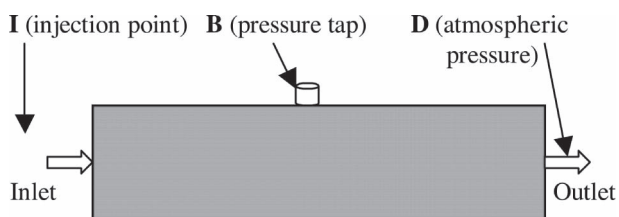


Fig. 4—Schematic charts of sandpacked models.

TABLE 2—CORE PARAMETERS OF SANDPACKED TUBES

| Quartz Size (Mesh) | Permeability (Darcy) | Pore Volume (cm ³) | Porosity (%) | Average Pore Diameter (μm) |
|--------------------|----------------------|--------------------------------|--------------|----------------------------|
| 20~40 | 65 | 51.14 | 44.9 | 82 |
| 40~60 | 39 | 50.51 | 44.3 | 64 |
| 60~80 | 24 | 50.32 | 44.1 | 51 |
| 80~100 | 16 | 49.86 | 43.7 | 43 |

Note: Tube diameter is 2.2 cm, and length is 30 cm.



Fig. 5—Two modes of particles through porous media (direct pass and retention).

Experimental Results

Propagation of PPG Through Porous Media. Visual micro-model experiments were carried out to observe PPG propagation through porous media. The weak particle sample (Sample 1) was used for all the micromodel experiments. After the particles were completely swollen, 5.0 cm³ of PPG suspension with a concentration of 0.1% was injected into the micromodels, and then tap water was injected into the model. The particle-transportation processes were monitored by video recorder during the injection of PPG suspension and followed water.

Fig. 5 shows two pictures of weak particles through a simplified regular micromodel in which pore-throat diameter in the first line is larger than the PPG particle average diameter. The average diameter of injected particles is 150 μm, which is between the pore-throat diameters of Line 1 (250 μm) and Line 2 (90 μm). As shown in this figure, most small particles can pass through the first line; we refer to this behavior as “direct flow” mode. Also, we can see that some particles are still left behind the first line, which is called “adsorption” mode. These retained particles are primarily located between the main flow paths and exhibit little retention in the main flow paths. This indicates that adsorption is related to the displacement pressure gradient. The reason for retention can be explained by the particle charge, which results in the attractive force between the particle and glass surface. Although adjusting the salinity of water can control particle adsorption/retention density, it is hard to eliminate it.

Fig. 6 shows the progress of a particle through a pore throat at an irregular micromodel when the particle is larger than the throat size. Four consecutive processes were monitored. First, the particle moved to the throat entrance, shown in **Fig. 6a**. Second, the particle changed its original shape when displaced by flowing water. It also was found that some water was squeezed from the swollen particle, which caused the swollen particle to shrink somewhat, as shown in **Fig. 6b**. Third, the particle was stretched to a long elliptic shape, like an amoeba, as shown in **Fig. 6c**. Finally, the particle suddenly passed through the pore at the displacement of water, and its original shape was partially restored, as shown in **Fig. 6d**.

Fig. 6 also illustrates the processes of particles through throats when the particles are greater than pore throats, but this experiment was performed at a specified regular model. Six consecutive procedures were recorded in the experiment shown in **Fig. 7**. It can be seen that some particles passed through pore throats smaller than their own sizes; some particles were retained and were blocked at the pore-throat entrance, and some particles were broken into smaller particles, then passed through the pore throat. If we focus on the processes of one particle through the throat(s), as circled on the six pictures, we can see the follow process. At first, a particle moved to the entrance of a throat and tried to pass through it, shown in **Fig. 7a**. Second, the particle was broken into two particles; the smaller one in front passed through the throat, then entered the pore space, as shown in **Fig. 7b**, and the larger part still blocked the throat, as shown in **Fig. 7c**. Third, the larger remaining part still had the ability to deform, and its shape became arched and blocked two throats, as shown in **Fig. 7d**. Fourth, two ends of the arched shape, significantly distorted, entered the two throats, as shown in **Fig. 7e**. Finally, the larger particle broke into two particles again. Compared to the broken particles with throat(s), it also can be seen that its size is still larger than the throat that it passed through.

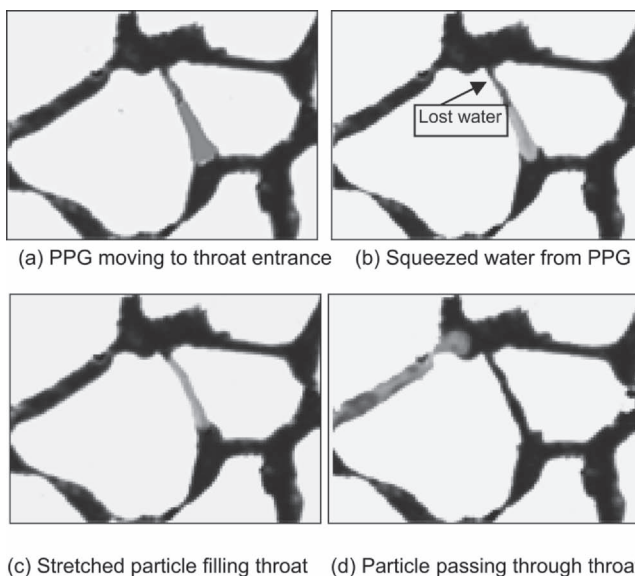


Fig. 6—A process of a particle through a throat.

The transport behavior of PPG particles through a porous medium can be summarized in six patterns as follows:

Direct Pass: A particle can move through a pore throat when displaced by water. This often happens when a particle is smaller than a pore throat.

Adsorption: Some particles are adsorbed/retained onto a porous-media surface. Adsorption often happens when the particle is

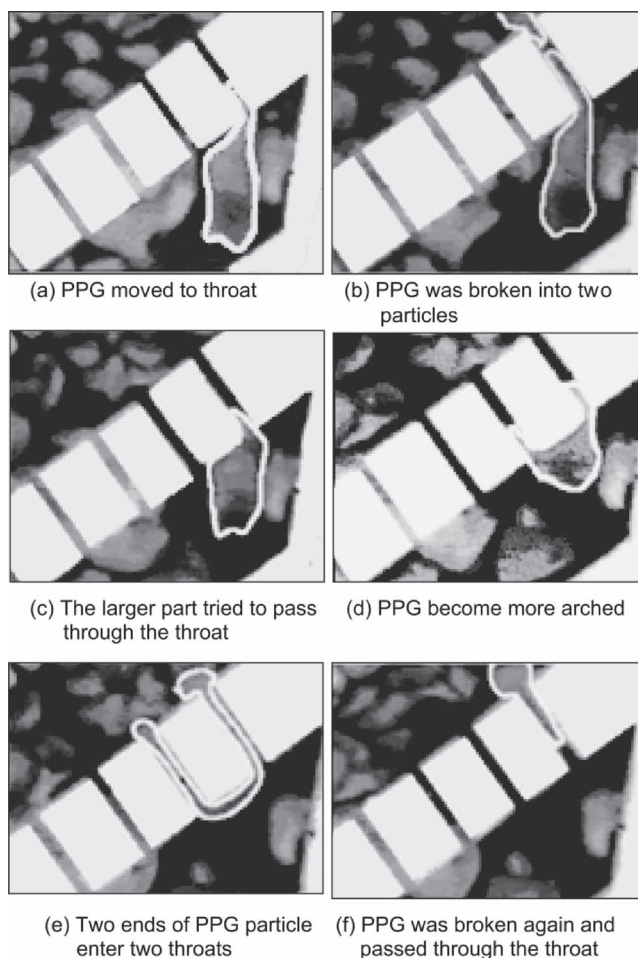
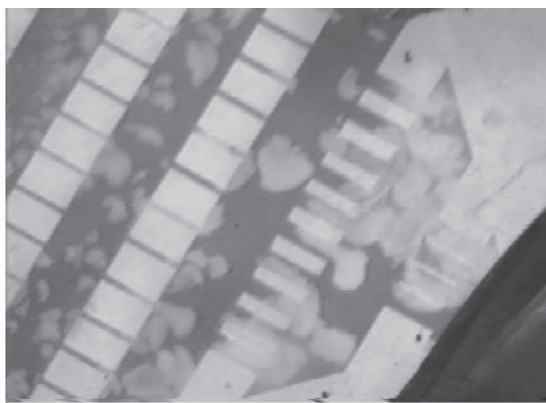
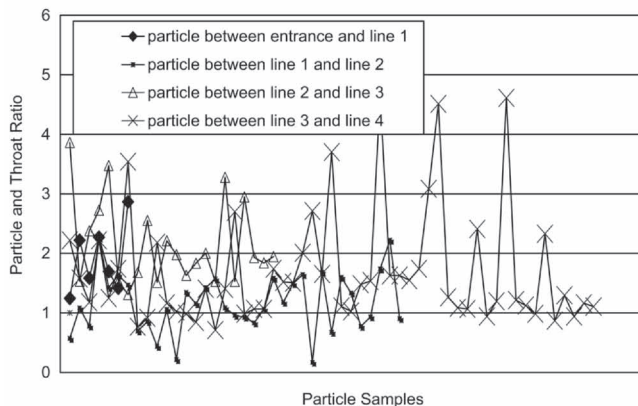


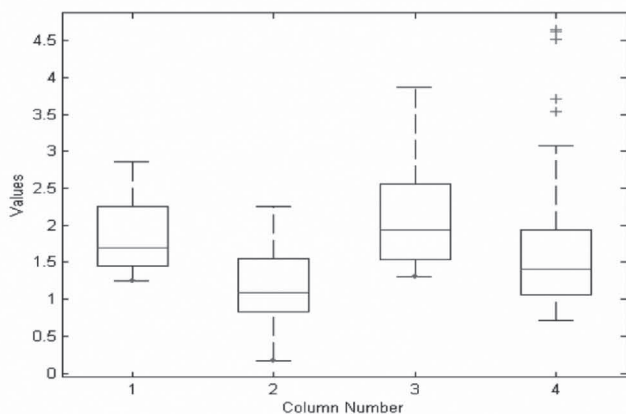
Fig. 7—A process of particles through throats at the simplified model.



(a) A typical visual experiment result photograph



(b) Particle sample distribution



(c) The box plot of diameter ratios and space between two lines

Fig. 8—Matching diameter ratios of particles and throats.

so small that the attraction force between rock surface and PPG surface is dominant.

Trap: A particle is blocked at the entrance of a pore throat and cannot move forward.

Deform and Pass: A particle changes its shape because of the displacement force applied by flowing water and passes through a throat. The deformed particle may revert to its original shape after entering a larger pore.

Shrink and Pass: Some water is squeezed from a swollen particle owing to the displacement force of water injection, and the shrunken particle can pass through the throat because of its decreased size. After the shrunken particle enters the pore, it may reabsorb some water from the pore space and revert to its original size.

Snap-Off and Pass: A particle is broken into smaller particles by a pore throat, and the smaller particles continue to pass through pore throats.

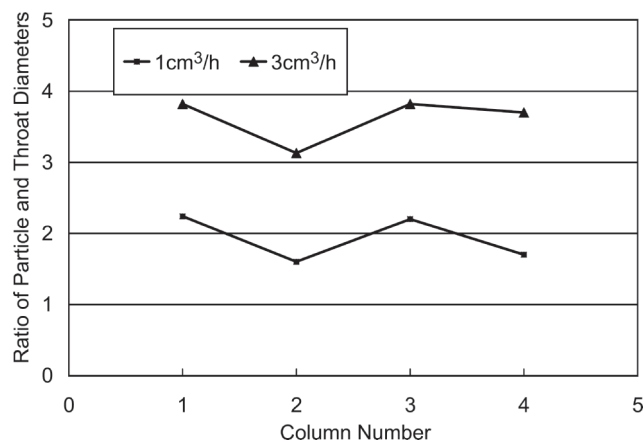


Fig. 9—Effect of injection rate on the matching ratio of the particle and throat diameters.

The last four patterns happen when a particle size is larger than a pore-throat size. In practice, several patterns often occur simultaneously when PPG moves through porous media. Also, the dominant pattern depends mainly on the diameter ratio of the swollen PPG particle and the pore throat, the strength of the swollen PPG, and the fluid driving force.

Matching Ratio of Particle and Pore Size. *Micromodel Experiments.*

The specific designed micromodels were used to study what size particle can pass through what size pore throat. Weak PPG particles with an average diameter of $150 \mu\text{m}$ were injected into the micromodels. Fig. 8a shows a typical result. Fig. 8b showed the ratios of average particle diameter in each column and throat diameter in the line behind the corresponding column. The ratios are mainly distributed from 2 to 4, which indicates that a particle can pass through a pore throat that is only one-quarter of the particle diameter. It should be noted that no particle with a diameter larger than five times the size of a throat diameter was observed because those large particles were broken into smaller particles, and the measured particles were only those that passed through the throats. So it can be inferred that some larger particles can also be injected into porous media but will be broken into smaller particles, and these new particles can continue to propagate through porous media. Fig. 8c shows the box plot for these data. The diameters of 25% particles are more than 2.8 times the first line-throat diameter, the diameters of 50% particles are more than 1.6 times the first line-throat diameter, and the diameters of 25% particles are less than 1.3 times the first line-throat diameter (Fig. 8c). The reason that some larger particles are left behind the first line is that these particles are so large that the fluid driving force from the experiment could not move them. The actual diameters of some particles are larger than $150 \mu\text{m}$ because $150 \mu\text{m}$ refers to the average diameter of the particles in the sample, but not their practical diameters.

Fig. 9 shows the effect of the injection rate on the ratio of a particle and a throat diameter. The measured particle sizes are more than two times the throat diameter at a flow rate of $1 \text{ cm}^3/\text{h}$, but they become more than three times the throat diameter at a flow rate of $3 \text{ cm}^3/\text{h}$. The main reason is that the higher flow rate has a higher driving force, and the higher driving force can make particles more deformable and, thus, more easily passed through pore throats. It also can be seen that the average particle-/throat-diameter ratio between the entrance and the first line are larger than that between any other two adjacent lines. This occurs because many larger particles are retained behind the first line.

Sandpacked Coreflooding Experiments (Macro-phenomena).

These experiments were performed to deduce particle propagation patterns through porous media at macroscopic scale. Sandpacked core models were used to evaluate swollen PPG propagation through porous media. In these experiments, a $1,000 \text{ mg/L}$ particle

| | Quartz size (mesh) | 20~40 | | 40~60 | | 60~80 | | 80~100 | |
|-------------------------|------------------------------------------------|-------|-----|-------|-----|-------|-----|--------|------|
| | Average pore diameter (μm) | 82 | | 64 | | 51 | | 43 | |
| Particle before swollen | Particle size (μm) | 60 | 90 | 60 | 90 | 60 | 90 | 60 | 90 |
| | Ratio of particle and pore | 0.7 | 1.1 | 0.9 | 1.4 | 1.2 | 1.8 | 1.4 | 2.1 |
| Particle after swollen | Ratio of particle and pore for weak particle | 3.5 | 5.7 | 4.7 | 7.0 | 5.9 | 8.8 | 7.7 | 11.6 |
| | Ratio of particle and pore for strong particle | 1.3 | 2.6 | 1.8 | | | | | |

suspension was injected until the injection pressure was stable or up to 3 MPa, which was the maximum available injection pressure. The injection rate was 1 cm³/min. The pressure changes at the injection point I and the middle point B were recorded during the injection. After the PPG suspension was injected, water was injected at a flow rate of 0.05 cm³/min until the pressures at all points were stabilized. The stabilized pressure was used to calculate the residual resistance factor.

Table 3 shows the ratios of the average pore diameter of porous media to the average particle diameter. Three parameters were used to analyze particle-propagation patterns: pressure change with time for each pressure tap, effluent particle size, and residual resistance factors of two segments for each model. **Table 4** summarizes the experimental results. Our results show that the particle propagation through porous media exhibits three patterns: pass, broken and pass, and plug. The characteristics of the different patterns are described as follows:

Pass: Injection pressure increases linearly at the beginning of PPG injection. When the volume of the particle suspension is injected to some amount, the pressure does not change any more, and a plateau appears, indicating a stable status. **Fig. 10** shows a typical pressure-change curve with time. From the figure, it can be seen clearly that the pressure changes at different taps have a similar trend, and a steady-state pressure can be read. The effluent particle size is the same as the injected particle size, as shown in **Figs. 11a and 11b** and **Table 5**. The effluent particle concentration is also the same as the injected, shown in **Table 5**. The residual resistance factor F_{rrs} is the same at different segments, as shown in **Table 6**. The F_{rr} was measured at the flow rate of 1 cm³/min.

Broken and Pass: The pressure-variation trend is the same as the “pass” pattern, but compared with the injected particle, the effluent particle size and concentration decreased, as shown in **Fig. 11c** and **Table 5**. The F_{rr} in the first segment was higher than that in the second segment, and the F_{rr} in the second segment was still much greater than 1, which indicates that some particles moved to this segment and flow resistance built up.

Plug: The injection pressure increases rapidly until it reaches the maximum available pressure, but the pressure in the middle tap

does not change; it stays almost the same as the pressure of the water injection before PPG injection, shown in **Fig. 12**. If the pressure is converted to resistance factor (F_r), the first segment F_r quickly increases from one to several hundreds, or even thousands, but the second segment F_r almost remains at one, which indicates that no particle passes through the second point. The core section was cut after experiments; it was found that all particles were packed in the inlet of the core, and most of them were squeezed to form a gel cake. No particle penetrates into the depth of the core; no particle is produced from the outlet of the core at all. The F_{rr} in the first segment is very high, but the F_{rr} in the second segment remains at one. This indicates that no particle reached the second segment. In general, for the “plug” pattern, particles filter cake at the core face, and only filtrate can pass through the core.

In summary, although PPG is deformable, its movement is limited by core permeability and PPG properties. For the same-size particle, a higher-strength gel causes a higher injection pressure; for the same gel strength, a smaller pore size results in a higher injection pressure.

In the experiments, a threshold pressure, defined as the pressure that causes the particle to move through a porous medium, was also measured. In other words, the particle can move through a porous medium only if the driving pressure is higher than the threshold pressure. **Fig. 13** shows the relationship of the threshold pressure and the diameter ratio of particle and average pore size. Two regions can be observed for weak particles in the figure. The threshold pressure in the first region increases sharply with the particle/pore diameter ratio, but in the second region, it increases quite slowly when the ratio is above 3. This occurs because a larger particle can be broken into small ones at higher pressure, and these small particles can pass through the pore throat. In field applications, it often has been found that the injection pressure was not sensitive to particle size when particle diameter was large to a value, and increased particle sizes did not increase injection pressure in some field applications. The experimental result may explain the field response. Weak particles have the same behavior as strong particles when the pressure is not enough to make the weak particles deform or crush.

| Particle | Weak Particle | | | | | | | | Strong Particle | | | |
|----------|-----------------------------------|---------|-----------------|---------|-----------------|---------|----------------|---------|-----------------|--|----|--|
| | 60 | | | | 90 | | | | 60 | | 90 | |
| | Particle size before swollen (μm) | Pattern | Pressure (MPa) | Pattern | Pressure (MPa) | Pattern | Pressure (MPa) | Pattern | Pressure (MPa) | | | |
| 20~40 | Pass | 0.012 | Broken and pass | 0.25 | Pass | 0.028 | Plug | >3 | | | | |
| 40~60 | Broken and pass | 0.25 | Plug | >3 | Broken and pass | 0.24 | Plug | >3 | | | | |
| 60~80 | Broken and pass | 1.20 | Plug | >3 | Plug | >3 | Plug | >3 | | | | |
| 80~100 | Plug | >3 | Plug | >3 | Plug | >3 | Plug | >3 | | | | |

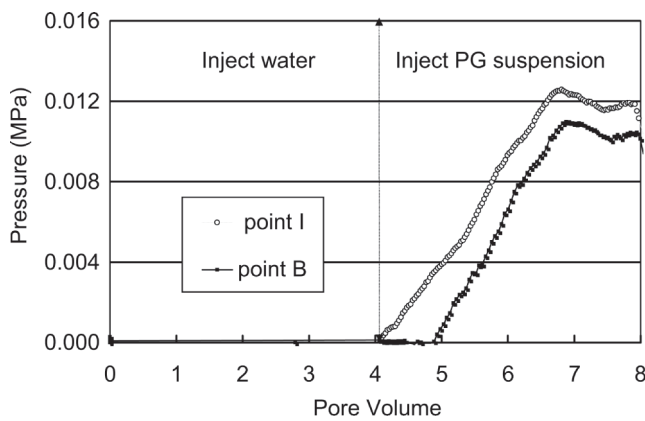


Fig. 10—A typical pressure curve for the “pass” and “broken and pass” patterns.

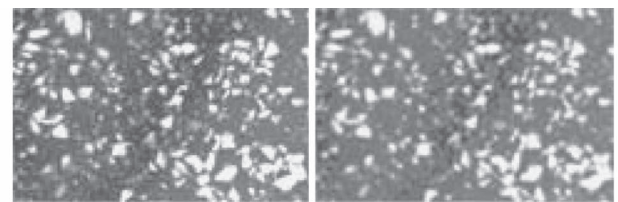
Discussion

Comparison of Normal Particles and PPG Particles. Prior to this study, extensive research was carried out to study the matching diameter ratio of a normal particle and a pore throat, such as clay or cement (Maroudas 1966; Pautz et al. 1989). The results are as follows:

- If $D_{\text{particle}} > 1/3 D_{\text{pore throat}}$, particles will form an external cake at the inlet of core, and this cake will prevent other particles from entering the core; thus, particles will only plug the core face.
- If $3D_{\text{particle}} < D_{\text{pore throat}} < 10D_{\text{particle}}$, particles will partially enter the core and form an internal cake, but the penetration depth is only several centimeters.
- If $10D_{\text{particle}} < D_{\text{pore throat}}$, the particle will move through the core until it exits the core or is trapped in the core.

The particles in this study are different from normal or hard sphere nondeformable particles in two ways. First, PPG particles can swell when mixed with water or brine. Second, swollen PPG particles are elastic and deformable, so they can pass easily through porous media. From our micromodel experiments, the swollen weak particle can pass through a pore throat with a diameter that is only a quarter of the swollen particle diameter. From the sandpacked model experiments, shown in Tables 3 and 4, the weak swollen particle can pass through a pore throat with a diameter that is only 0.175 (1/5.7) times the size of its own diameter, and a dry PPG particle can pass through a pore throat 0.83 times its own diameter. The strong swollen particle can pass through the throat with a diameter only 0.78 (1/1.3) times the size of its own diameter, in which the diameter of its dry PPG particle is 0.7 times the pore diameter. The injection-pressure gradients from the sandpacked experiments are higher than those from the micromodel experiments.

Particle Injectivity. Although a swollen PPG particle is elastic and deformable and is easier to move through a porous medium than a normal particle, the deformability and elasticity is limited. Our sandpack experiments demonstrate that a particle with a diameter of 60 μm cannot pass through porous media with a permeability of 16 D, as shown in Tables 4 and 5. In our lab, experiments also demonstrate that PPG particles visible to the naked eye cannot enter consolidated porous media with permeability less than 1 D. In other words, a commercially available PPG product cannot be injected into matrix resulting from the formation of face



(a) PPG particles before injected (b) PPG effluent from “pass” pattern



(c) PPG effluent from “broken and pass” pattern

Fig. 11—Particle size and concentration variations before and after PPG passed through porous media.

plugging on the core surface. Commercially available PPG can be injected only into fractured rocks or porous media with super high permeability.

However, although injectivity is a major problem in the laboratory, no injectivity problems were found in most field applications (Liu et al. 2006). For those fractured reservoirs, the results can be explained easily. But for those reservoirs without initial fractures or purposely hydraulic fractures, a reasonable explanation is that high-permeability channels have been formed in the mature oil fields during long periods of waterflooding. Such channels are currently undetectable.

Particle Retention in Porous Media. Our micromodel experiments show that some particles will remain in some pore spaces or block some pore throats. These particles will reduce water permeability by blocking some or all flow paths. In other words, trapped or retained particles will reduce the void volume of the porous medium available for flow. Thus, higher residual flow resistances are often measured in the laboratory. Sometimes, the stationary particle will act as a weak, flexible pore wall to divert fluid flow if adequate pressure is present. For a two-phase system of oil and water, additional experiments need to be performed to determine the effects of PPG on oil and water permeability. Such experiments will aid in understanding PPG treatment mechanisms.

Particle Flow Through Porous Media. The viscosity of particle suspension with a concentration of 1,000 mg/L is the same as water if it is measured with a viscometer. However, injection of particle suspensions showed a higher resistance in the experiments than water because the particles that flow through a porous medium contribute extra resistance to transport. An effective viscosity term can be used to describe the unusual resistance.

During particle flow through porous media, most particles do not maintain their identities over macroscopic distances. Rather, they break and deform by the pore-level “breaking and changing” processes. In addition, the behavior of a particle through porous media is intimately related to the connectivity and geometry of the medium in which it resides.

TABLE 5—COMPARISON OF INJECTION AND EFFLUENT PPG PARTICLE DIAMETER

| Patterns | Diameter of Weak Particles | | Diameter of Strong Particles | |
|-----------------|----------------------------|----------|------------------------------|----------|
| | Injection | Effluent | Injection | Effluent |
| Pass | 0.236 | 0.226 | 0.160 | 0.156 |
| Broken and Pass | 0.236 | 0.193 | 0.160 | 0.121 |
| Plug | 0.236 | — | 0.160 | — |

| TABLE 6—RESISTANCE FACTOR (F_r) AND RESIDUAL RESISTANCE FACTOR (F_{rr}) OF DIFFERENT SEGMENTS | | | | | |
|-------------------------------------------------------------------------------------------------------|-------------|------------------|----------|------|-----------------|
| Particle No. | Quartz Size | PG Particle Size | F_{rr} | | Pattern |
| | | | IB | BD | |
| 1 | 20–40 | 250 | 6.4 | 6.3 | Pass |
| 2 | 20–40 | 250 | 6.9 | 6.3 | |
| 1 | 20–40 | 160 | 77.4 | 43.6 | |
| 1 | 40–60 | 250 | 31.3 | 12.3 | Broken and Pass |
| 1 | 60–80 | 250 | 20.6 | 15.9 | |
| 2 | 40–60 | 250 | 96.1 | 57.1 | Plug |
| 1 | 40–60 | 160 | 230 | 1.3 | |
| 1 | 60–80 | 160 | 127 | 1.0 | |
| 1 | 80–100 | 250 | 177 | 1.0 | |
| 2 | 20–40 | 160 | 519 | 1.2 | |
| 2 | 40–60 | 160 | 299 | 1.0 | |

Future Work

Although some research on PPG has been carried out, such as the synthesis, property evaluation, and evaluation of transport mechanisms through porous media (as done in this study), additional work needs to be done to further evaluate the effectiveness of this technology. Further work in our laboratory will focus on two topics:

- Determine which information is more instructive for particle selection. Proper selection of particle size, strength, mass, and PPG suspension concentration will aid in improving the results of PPG applications. Economic constraints suggest that knowing what information is most effective for PPG selection is the best approach.

- Model PPG transport through porous media. This will aid in designing and forecasting PPG treatment.

Improving the Oil-Recovery Mechanisms of PPG Treatments. As we know, the recovery efficiency can be calculated from the following formula:

$$E_R = E_D \times E_A \times E_I, \dots \dots \dots (1)$$

where E_R =recovery efficiency, E_D =displacement efficiency, E_A =areal sweep efficiency, and E_I =vertical sweep efficiency. Therefore, experiments will be carried out to determine whether PPG has the potential to improve vertical sweep efficiency, aerial sweep efficiency, displacement efficiency, and determination of the improved-oil-recovery mechanism for PPG.

Optimize PPG Treatment Design. To optimize PPG treatment design, we will:

- Know our reservoirs. Understanding what has happened in the past for a reservoir and its current status is a key to improved-oil-recovery method selection. Knowing current reservoir status aids in explaining the injectivity “conflict” between laboratory experiments and field applications because most field applications have shown no injectivity problem at all, even though the reservoirs have no natural fractures or intentional hydraulically induced fractures.

Conclusions

1. At the microscopic scale, PPG propagation through pore throats exhibits six patterns: direct pass, adsorption, deform and pass, snap-off and pass, shrink and pass, and trap.
2. At the macroscopic scale, PPG propagation through porous media can be described by three patterns: pass, broken and pass, and plug. The dominant pattern can be determined by three parameters: pressure change with time at different taps, comparison of injected and produced particle size, and residual resistance factors at different segments of a core.
3. A swollen PPG particle can pass through a pore throat with a diameter that is much smaller than the swollen PPG diameter. The weaker the swollen particle is, the larger the particle that can pass through a pore throat.
4. PPG can move through porous media only if a driving pressure gradient is larger than a threshold pressure gradient. The magnitude of a threshold pressure depends on the particle size, strength, and pore-throat structure of the porous medium.
5. PPG retention in porous media can be described by the permeability reduction of a porous medium. The PPG flow through porous media can be described by an effective viscosity.

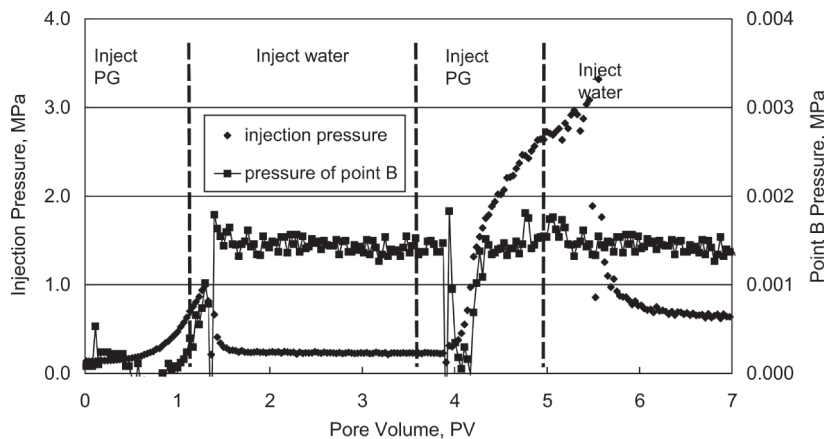


Fig. 12—A typical pressure curve for the “plug” pattern.

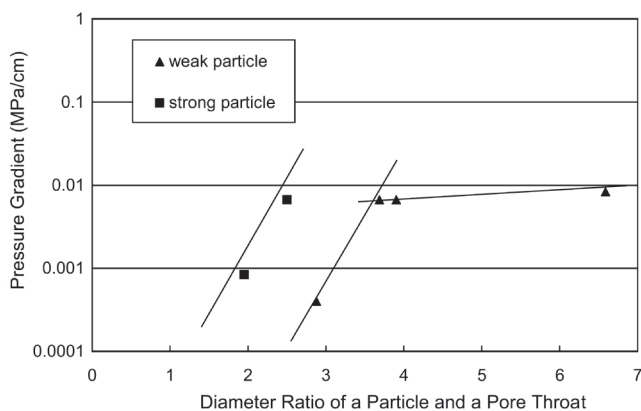


Fig. 13—Effect of the diameter ratio of a particle and a pore throat on the threshold pressure gradient.

Nomenclature

- D_{particle} = diameter of a particle, mm
 $D_{\text{pore throat}}$ = diameter of a pore throat, mm
 E_A = areal sweep efficiency
 E_D = displacement efficiency
 E_I = vertical sweep efficiency
 E_R = recovery efficiency
 S_{circle} = area of a circle
 S_{particle} = area of a circle

Acknowledgments

Financial support for this work is gratefully acknowledged from the China Ministry of Science and Technology (the Natl. High Technology Research and Development Programs of China—863 Program), Petro-China Co. Ltd., China Natl. Petroleum Corp. (CNPC), China Natl. Offshore Oil Corp. (CNOOC), China Petroleum and Chemical Corp. (SINOPEC), and Daqing Oil Co. Ltd. We also thank Mike Whitworth (U. of Missouri-Rolla) and Randy Seright and Reid Grigg (New Mexico Petroleum Recovery Research Center) for their helpful suggestions.

References

- Bai, B., Li, L., Liu, Y., Wang, Z., and Liu, H. 2004. Preformed Particle Gel for Conformance Control: Factors Affecting its Properties and Applications. Paper SPE 89389 presented at the SPE/DOE Symposium on Improved Oil Recovery, Tulsa, 17–21 April. DOI: 10.2118/89389-MS.
- Bai, B., Li, Y., and Liu, X. 1999. New Development of Water Shutoff and Profile Control in Oilfields in China. *Oil Drilling & Production Technology* **20** (3): 64–68.
- Chambers, K.T. 1990. Capillary pore-level basics for modeling foam flow in porous media with randomly connected pore throats and bodies. MS thesis, U. of California, Berkeley, California.
- Chauveteau, G., Omari, A., Tabary, R., Renard, M., Veerapen, J., and Rose, J. 2001. New Size-Controlled Microgels for Oil Production. Paper SPE 64988 presented at the SPE International Symposium on Oilfield Chemistry, Houston, 13–16 February. DOI: 10.2118/64988-MS.
- Chauveteau, G., Omari, A., Tabary, R., Renard, M., and Rose, J. 2000. Controlling Gelation Time and Microgel Size for Water Shutoff. Paper SPE 59317 presented at the SPE/DOE Improved Oil Recovery Symposium, Tulsa, 3–5 April. DOI: 10.2118/59317-MS.
- Chauveteau, G., Tabary, R., Le Bon, C., Renard, M., Feng, Y., and Omari, A. 2003. In-Depth Permeability Control by Adsorption of Weak Size-Controlled Microgels. Paper SPE 82228 presented at the SPE European Formation Damage Conference, The Hague, 13–14 May. DOI: 10.2118/82228-MS.
- Coste, J.P., Liu, Y., Bai, B. et al. 2000. In-Depth Fluid Diversion by Pre-Gelled Particles. Laboratory Study and Pilot Testing. Paper SPE 59362 presented at the SPE/DOE Improved Oil Recovery Symposium, Tulsa, 3–5 April. DOI: 10.2118/59362-MS.
- Feng, Y., Tabary, R., Renard, M., Le Bon, C., Omari, A., and Chauveteau, G. 2003. Characteristics of Microgels Designed for Water Shutoff and Profile Control. Paper SPE 80203 presented at the SPE International

- Symposium on Oilfield Chemistry, Houston, 5–7 February. DOI: 10.2118/80203-MS.
- Fielding, R.C. Jr., Gibbons, D.H., and Legrand, F.P. 1994. In-Depth Drive Fluid Diversion Using an Evolution of Colloidal Dispersion Gels and New Bulk Gels: An Operational Case History of North Rainbow Ranch Unit. Paper SPE 27773 presented at the SPE/DOE Improved Oil Recovery Symposium, Tulsa, 17–20 April. DOI: 10.2118/27773-MS.
- Grigg, R.B. and Schechter, D.S. 1997. State of the Industry in CO₂ Floods. Paper SPE 38849 presented at the SPE Annual Technical Conference and Exhibition, San Antonio, Texas, 5–8 October. DOI: 10.2118/38849-MS.
- Lane, R.H. and Seright, R.S. 2000. Gel Water Shutoff in Fractured or Faulted Horizontal Wells. Paper SPE 65527 presented at the SPE/CIM International Conference on Horizontal Well Technology, Calgary, 6–8 November. DOI: 10.2118/65527-MS.
- Liu, Y., Bai, B., and Shuler, P.L. 2006. Application and Development of Chemical-Based Conformance Control Treatments in China Oil Fields. Paper SPE 99641 presented at the SPE/DOE Symposium on Improved Oil Recovery, Tulsa, 22–26 April. DOI: 10.2118/99641-MS.
- Liu, Y., Bai, B., and Li, Y. 1999. Research on Preformed Gel Grains for Water Shutoff and Profile Control. *Oil Drilling & Production Technology* **21** (3): 65–68.
- Maroudas, A. 1966. Particle Deposition in Granular Filter Media-2. *Filtration and Separation* **3** (2): 115–121.
- Morrow, N.R. 1991. *Interfacial Phenomena in Petroleum Recovery*. New York City: Marcel Dekker Inc.
- Pautz, J.F., Crocker, M.E., and Walton, C.G. 1989. Relating Water Quality and Formation Permeability to Loss of Injectivity. Paper SPE 18888 presented at the SPE Production Operations Symposium, Oklahoma City, Oklahoma, 13–14 March. DOI: 10.2118/18888-MS.
- Seright, R.S. 1997. Use of Preformed Gels for Conformance Control in Fractured Systems. *SPEPF* **12** (1): 59–65. SPE-35351-PA. DOI: 10.2118/35351-PA.
- Seright, R.S. 2000. Gel Propagation Through Fractures. Paper SPE 59316 presented at the SPE/DOE Improved Oil Recovery Symposium, Tulsa, 3–5 April. DOI: 10.2118/59316-MS.
- Seright, R.S. 2003. Washout of Cr (III)-Acetate-HPAM Gels From Fractures. Paper SPE 80200 presented at the SPE International Symposium on Oilfield Chemistry, Houston, 5–7 February. DOI: 10.2118/80200-MS.
- Song, W., Yang, C., Han, D., Qu, Z., Wang, B., and Jia, W. 1995. Alkaline-Surfactant-Polymer Combination Flooding for Improving Recovery of the Oil With High Acid Value. Paper SPE 29905 presented at the SPE International Meeting on Petroleum Engineering, Beijing, 14–17 November. DOI: 10.2118/29905-MS.
- Sydansk, R.D. 1988. A New Conformance-Improvement-Treatment Chromium (III) Gel Technology. Paper SPE 17329 presented at the SPE/DOE Enhanced Oil Recovery Symposium, Tulsa, 16–20 April. DOI: 10.2118/17329-MS.
- Sydansk, R.D. and Southwell, G.P. 2000. More Than 12 Years' Experience With a Successful Conformance-Control Polymer-Gel Technology. *SPEPF* **15** (4): 270–278. SPE-66558-PA. DOI: 10.2118/66558-PA.
- Wang, D., Zhao, L., Cheng, J., and Wu, J. 2003. Actual Field Data Show That Production Costs of Polymer Flooding Can Be Lower Than Water Flooding. Paper SPE 84849 presented at the SPE International Improved Oil Recovery Conference in Asia Pacific, Kuala Lumpur, 20–21 October. DOI: 10.2118/84849-MS.
- Wang, H.G., Guo, W.K., and Jiang, H.F. 2001. Study and Application of Weak Gel System Prepared by Complex Polymer Used for Depth Profile Modification. Paper SPE 65379 presented at the SPE International Symposium on Oilfield Chemistry, Houston, 13–16 February. DOI: 10.2118/65379-MS.

SI Metric Conversion Factors

| | |
|------------------------------|------------------------|
| atm × 1.013 250* | E+05 = Pa |
| °F (°F–32)/1.8 | = °C |
| in. × 2.54* | E+00 = cm |
| in. ³ × 1.638 706 | E+01 = cm ³ |

*Conversion factor is exact.

Baojun Bai is an assistant professor at the U. of Missouri-Rolla. e-mail: baib@umr.edu. Previously, he was head of the conformance control section at the Research Inst. of Petroleum Exploration and Development (RIPED), PetroChina. Bai also was a post-doctoral scholar at the California Inst. of Technology (Caltech) and a graduate research assistant at the New Mexico Petroleum Recovery Research Center (PRRC). He holds a BS degree in reservoir engineering, an MS degree in oil and gas production and development engineering, and PhD degrees in petroleum engineering and in geosciences. **Yuzhang Liu** is a vice president and research professor at RIPED, PetroChina. He has been working on production technology development and research project management in-

volving improved oil recovery, enhanced oil recovery, stimulation, water control, and sand control. Liu holds a bachelor's degree in petroleum engineering. **Jean-Paul Coste** was a post-doctoral student at RIPED. He holds a PhD degree in petroleum engineering from the Inst. Français du Pétrole. **Liangxiang Li** is currently a research scientist at the New Mexico PRRC. His research focuses on developing novel membranes for produced-water purification and water control. Li worked for Petro-China as a research engineer in water shutoff before joining the PRRC. He holds a BS degree in chemistry science from Hubei U., an MS degree in petroleum engineering from RIPED, and a PhD degree in material engineering from the New Mexico Inst. of Mining and Technology.